Concurrent Design of Linear Control with Input Shaping for a Two-Link Flexible Manipulator Arm

Daniel Newman * **Joshua Vaughan** *

* *Department of Mechanical Engineering, University of Louisiana at Lafayette, Lafayette, Louisiana 70504 USA (e-mail: joshua.vaughan@louisiana.edu).*

Abstract: Input shaping is an effective vibration control technique for flexible systems with known dynamic characteristics. However, due to its open-loop nature, it must be combined with a feedback controller to enable rejection of unknown disturbances. Although a number of researchers have demonstrated the effectiveness of combining input shaping and feedback control methods, performance gains can be made by cooperatively designing the feedback gains and input shaping sequence. This paper presents a preliminary investigation of such a control method on a two-link flexible manipulator. This formulation allows for energy-efficient point-to-point motion while simultaneously minimizing command-induced vibration. Simulations demonstrate the effectiveness of this preliminary work.

Keywords: Linear systems, Parametric optimization, Input and excitation design

1. INTRODUCTION

Increasing the productivity of flexible mechanical systems typically requires rapid point-to-point motion as well as disturbance rejection. Command shaping has been thoroughly shown to allow quick motion without exciting vibration [Singhose (2009)]. Specifically, input shaping is a widely used command shaping technique due to its simplicity and effectiveness. However, because input shaping is open-loop, it cannot be used to reject unmodeled disturbances. To do so, feedback control methods must be used.

A significant amount of effort has been given to incorporate input shaping with feedback control [Kapila et al. (1999); Yang et al. (2014); Chatlatanagulchai and Benjalersyarnon (2015); Stergiopoulos and Tzes (2010); Staehlin and Singh (2003); Vyhlídal et al. (2016); Huey et al. (2008); Sorensen et al. (2007)]. Commonly called "closed-loop input shaping," this approach places an input shaper within the feedback loop, permitting it to act directly on the plant. This implementation ensures that the control signal is always fully shaped. However, closed-loop input shaping mandates that the control gains be chosen to ensure stability subject to the time-delay caused by the input shaper [Huey and Singhose (2010)].

In each cited example of closed-loop input shaping, the input shaper and feedback gains were designed sequentially. Recent work indicates that placing an input shaper outside the feedback loop and concurrently designing the input shaper with the feedback gains shows promise as a control approach [Baheri and Vaughan (2015); Huey and Singhose (2012); Kenison and Singhose (2002); Muenchhof and Singh (2002)]. However, [Baheri and Vaughan (2015); Huey and Singhose (2012)], and [Kenison and Singhose (2002)] only consider the control of a point mass. A flexible system was considered in [Muenchhof and Singh (2002)], where robustness to parametric uncertainty was improved by utilizing full-state feedback control optimized concurrently with input shaping.

Because input shaping generates commands which do not excite oscillatory plant dynamics, it will result in more energy-efficient rest-to-rest commands than feedback control alone. Because the rigid-body motion generated by input shaping brings the system to rest, no additional energy is required to dampen residual vibration. Furthermore, by delaying a portion of the reference command, input shaping can reduce the peak actuator effort required to reach the desired states. If the closed-loop control gains are intelligently designed to maximize the advantages that input shaping provides, a control system with better performance than either method alone can be created.

This paper will expand on the concept of concurrently-designed input shaping and feedback control with an application to a two-link flexible manipulator. In a system with limited available actuator effort, the concurrent design approach will be used to generate commands which result in minimal rise time without exciting oscillatory dynamics. This method will be compared to Linear Quadratic Regulation (LQR) for settling time, required actuator effort, and disturbance rejection properties.

The next section will discuss the relevant properties of input shaping. Next, Section 3 will introduce the benchmark dynamic model and provide an analysis of its relevant dynamic properties. An optimal control law will be presented in Section 4. A benchmark comparison of the proposed control method to LQR is given through computer simulations in Section 5. Finally, concluding remarks are given in Section 6.

2. INPUT SHAPING OVERVIEW

Input shaping is a popular and effective open-loop control method which has been applied to a wide array of flexible systems [Singhose (2009); Singer and Seering (1990)]. With input shaping, vibration reduction can be achieved by designing a sequence of impulses, called an input shaper, which result in low oscillation when convolved with a reference command.

The residual vibration equation provides a fundamental constraint for formulating an input shaper with n impulses of amplitudes A_i and times t_i

$$V(\omega,\zeta) = e^{-\zeta\omega t_n}\sqrt{[C(\omega,\zeta)]^2 + [S(\omega,\zeta)]^2}, \tag{1}$$

where

$$C(\omega,\zeta) = \sum_{i=1}^{n} A_i e^{\zeta\omega t_i}\cos(\omega\sqrt{1-\zeta^2}t_i), \tag{2}$$

$$S(\omega,\zeta) = \sum_{i=1}^{n} A_i e^{\zeta\omega t_i}\sin(\omega\sqrt{1-\zeta^2}t_i), \tag{3}$$

and ω and ζ are the natural frequency and damping ratio of the shaped mode, respectively. Equation (1) gives the ratio of residual vibration for a series of impulses relative to a unity magnitude impulse at time $t = 0$. The simplest input shaper is given by setting (1) equal to zero while constraining all impulse amplitudes to be positive. After further specifying that the minimum-time result is desired, the result is the Zero Vibration (ZV) shaper [Smith (1957)], which has the form

$$\text{ZV} = \begin{bmatrix} A_i \\ t_i \end{bmatrix} = \begin{bmatrix} \frac{1}{1+K} & \frac{K}{1+K} \\ 0 & \frac{\tau_d}{2} \end{bmatrix}, \tag{4}$$

where

$$K = e^{\frac{-\zeta\pi}{\sqrt{1-\zeta^2}}}, \tag{5}$$

and τ_d is the damped oscillation period of the system.

Note that the settling time of a response subject to a shaped command is explicitly related to the time of the final impulse of the input shaper, t_n. Although a number of modifications to the constraint equations for an input shaper can be made [Vaughan et al. (2008)], t_n, and therefore the settling time, $t_{s,shaped}$, is always proportional to τ_d

$$t_{s,shaped} \propto \frac{\pi}{\omega\sqrt{1-\zeta^2}}. \tag{6}$$

This relationship between settling time and pole location is unique to input shaping. Because t_s of a second-order system is otherwise related to its time constant

$$t_s \propto \frac{1}{\omega\zeta}, \tag{7}$$

there exists a damping threshold beyond which input shaping increases the settling time of the response. For a 5% settling time, this value is $\zeta \approx 0.7$.

Another important metric of input shaper performance is robustness to modeling errors. This can be visualized by plotting (1) for a given shaper sequence subject to changing ω and ζ. An example sensitivity plot for a ZV shaper designed to cancel $\omega = 1$Hz and $\zeta = 0.05$ is shown in Fig. 1. Viewing cross-sections of this curve along the ζ axis results in the often referenced sensitivity curves used to evaluate input shaper robustness.

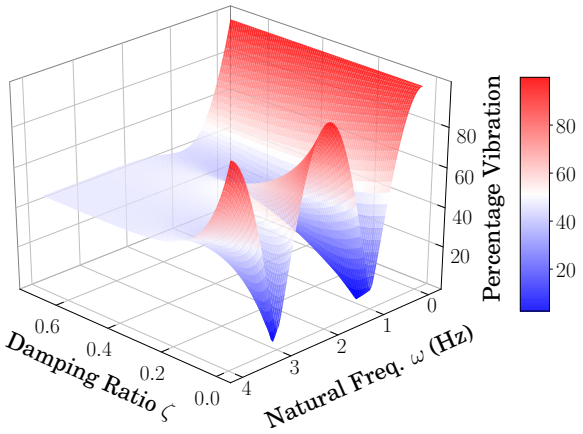

Fig. 1. Sensitivity plot for a ZV shaper

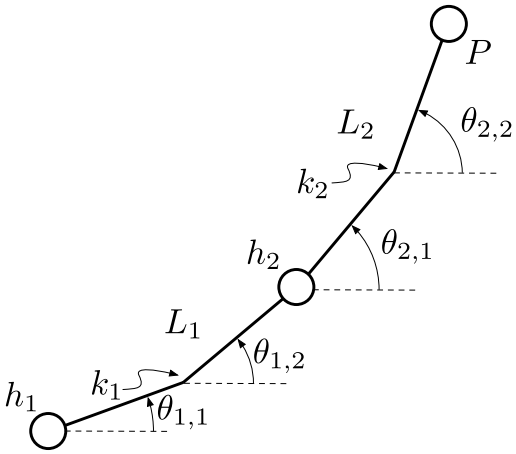

Fig. 2. Dynamic model of a two link flexible-arm manipulator

3. DYNAMIC MODEL

The dynamic model used in this analysis is shown in Fig. 2. The two-link flexible manipulator is modeled as a series of rigid bodies connected by rotational springs. Links L_1 and L_2 are rotated about hubs h_1 and h_2 and modeled by n elements. Each element, hub, and the payload P are modeled as homogeneous rigid bodies with corresponding masses and moments of inertia. The nodal displacements are given by

$$Q_{2n\times 1} = [\theta_{1,1}\ \theta_{1,2}\ \ldots\ \theta_{1,n}\ \theta_{2,1}\ \theta_{2,2}\ \ldots\ \theta_{2,n}]^T. \tag{8}$$

For each link with n elements, $n-1$ internal rotational springs are used to model the flexible behavior of the material. These springs are based on Euler-Bernoulli beam theory, which relates the internal bending moment to deflection by

$$\frac{M}{EI} = \frac{\mathrm{d}^2 y}{\mathrm{d}x^2}, \tag{9}$$

where E and I are the material modulus of elasticity and area moment of inertia, respectively. If small deflections

are assumed, the slope of the beam can be approximated by

$$\theta_{m,n} = \frac{\mathrm{d}y}{\mathrm{d}x}. \tag{10}$$

The stiffness of the i^{th} spring is therefore given by

$$k_i = \frac{EI}{2l_i}. \tag{11}$$

The resulting equations of motion were created by Kane's method using the Python SymPy module [Meurer et al. (2017)]. The state-space representation of the dynamic system is given by

$$\begin{bmatrix}\dot{Q}\\ \ddot{Q}\end{bmatrix} = \begin{bmatrix}0 & I\\ M^{-1}K & 0\end{bmatrix}\begin{bmatrix}Q\\ \dot{Q}\end{bmatrix} + Bu, \tag{12}$$

where,

$$B_{4n\times 2} = \begin{bmatrix}0_{2n\times 1} & 1 & 0_{(2n-1)\times 1}\\ 0_{3n\times 1} & 1 & 0_{(3n-1)\times 1}\end{bmatrix}^T, \tag{13}$$

and,

$$u = K\begin{bmatrix}Q\\ \dot{Q}\end{bmatrix}. \tag{14}$$

While the system model consists of n elements per link, the states at hubs h_1 and h_2 as well as the payload P are assumed to be observable. The resulting output matrix is given by

$$C_{4n\times 1} = [1\ 0_{n-2}\ 1\ \ldots\ 1\ 0_{n-2}\ 1]. \tag{15}$$

3.1 Eigenvalue Analysis

For the dynamic model considered in this work, the system has $2n$ unique eigenvalues, two of which are associated with the rigid body motion. In reality, an Euler-Bernoulli beam possesses a countably infinite number of modes due to the transcendental nature of its characteristic equation. However, the dominant dynamics can be accurately captured by considering one or two flexible modes. Because the model in this work has a finite number of elements, the calculated eigenvalues will be approximations of the true values. These approximations can be improved by increasing the number of elements at the cost of computational complexity.

In order to design an input shaper to eliminate vibratory modes for the two-link flexible manipulator, the eigenvalues of the state transition matrix in (12) should be evaluated. Having this knowledge of the system pole locations allows for time-efficient input shapers that eliminate the dominant modes to be designed. Because the eigenvalues are configuration-dependent, a nominal configuration must be chosen to generate the eigenvalues to be suppressed by the input shaper.

Although the eigenvalues of the two-link system are dependent on the configuration of the links, the variation is not exceptionally large. Figure 3 demonstrates the percent difference of the first four flexible modes of a model with $n = 4$ elements as a function of θ_2. As shown, the variation in frequency is less than 5% for the low modes. This difference becomes almost zero for high frequency modes.

4. CONTROL DESIGN

For the given system, a controller is desired which provides fast rise time subject to actuator constraints. This

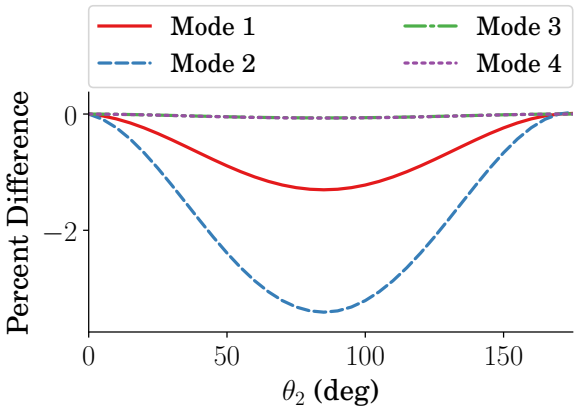

Fig. 3. Variation in frequency as a result of configuration change

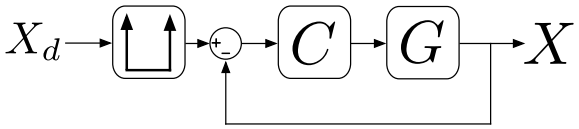

Fig. 4. Block diagram of the proposed control method

controller will utilize input shaping to modify the reference command outside of the feedback loop, while the feedback gains and input shaper are concurrently designed for optimal performance. The block diagram for this controller is shown in Fig. 4, which shows that the controller, C, acts on the plant, G, to push the system states to their desired values, X_d. These desired states are given by convolving the reference signal – in this case a step input – with an input shaper. Forming the controller in this way as opposed to a shaper-in-the-loop approach eliminates the need to consider possible instability caused by the time delay from the shaper impulses.

To provide a direct comparison between input shaping and optimal linear control, the gain matrix K will be selected by LQR. For the shaped command, the state and actuator weight matrices Q and R will be tuned by minimizing a cost function associated with the shaped step response properties. The cost function is given by

$$J = \alpha t_n^2 + \beta \int_{t_0}^{t_n} \left(\frac{1}{u(t)}\right)^2 \mathrm{d}t, \tag{16}$$

where

$$u(t) = K(x_d(t) - x(t)), \tag{17}$$

and the desired states, $x_d(t)$, are given by the convolution of a reference step input with the input shaper. This function penalizes the shaper duration and the inverse of the shaped actuator effort, respectively. The weights α and β can be modified to penalize these values differently. These terms were selected based on their contribution to the characteristics of the desired response. The duration of the input shaper serves as a proxy for command duration, which should be minimized. However, this term alone does not directly determine how aggressively the system will be pushed to the desired setpoint. To make this desired property explicit, the second term is added.

Table 1. System Parameters

Variable	Value
n	3
L_1, L_2	0.5m
ρ	$0.2\frac{\text{kg}}{\text{m}}$
m_p	0.1kg
m_{h1}	0kg
m_{h2}	1kg
J_{h1}, J_{h2}	0.1kg m^2
J_p	0.0005kg m^2
τ_{max}	10N·m
$\Delta\theta_1 = \Delta\theta_2$	90°

Equation (16) is minimized subject to the constraint that the peak actuator effort must not exceed the allowed torque

$$u_{max} \leq \tau_{max}. \tag{18}$$

Because input shaping will be used for the low modes, a constraint limiting their damping ratios will be enforced to ensure low settling time.

$$\zeta_{k,opt} \leq 0.7. \tag{19}$$

4.1 Input Shaper Design

Designing an input shaper for the multi-mode system under consideration requires knowledge of the dominant dynamics. The low frequency rigid-body modes are assumed to dominate the response characteristics of the two-link flexible manipulator relative to the flexible dynamics. Furthermore, shaping the low modes implicitly limits vibration in higher frequency modes if positive amplitude input shapers are used. The nature of the positive amplitude constraint strictly means that the worst case for high mode excitation will be an oscillatory response equal to that of an unshaped command.

For this preliminary work, a four-mode convolved ZV shaper will be used to eliminate the low frequency modes. This formulation allows the two rigid body modes and first two flexible modes to be shaped. Because the resulting multi-mode shaper is convolved, it is not time-optimal for the vibration constraints [Singhose et al. (1997)]. However, this shaping approach simplifies the optimization process.

5. EXAMPLE APPLICATION

Based on the proposed control approach, an example simulation using the parameters given in Table 1 was performed. The physical system characteristics were chosen to match those presented in [De Luca and Siciliano (1991)], while the number of elements $n = 3$ was chosen to be computationally efficient while yielding a sufficient number of modes for analysis. The state and input matrices for the benchmark LQR controller were tuned using the same cost function for an accurate comparison. Assuming that the intermediate states along each link are unobservable, the resulting control gains are

$$K_{LQR} = \begin{bmatrix} 7.16 & -6.87 \\ 0.0 & 0.0 \\ -0.19 & 2.46 \\ -0.57 & 13.78 \\ 0.0 & 0.0 \\ 0.09 & -3.25 \\ 3.75 & -1.31 \\ 0.0 & 0.0 \\ -0.08 & 1.40 \\ -0.15 & 5.29 \\ 0.0 & 0.0 \\ -0.11 & -0.06 \end{bmatrix}. \tag{20}$$

These control gains result in the following modal characteristics

$$\begin{bmatrix} \omega_{k,LQR} \\ \zeta_{k,LQR} \end{bmatrix} = \begin{bmatrix} 0.29 & 0.39 & 0.79 & 2.38 & 8.02 & 21.97 \\ 0.48 & 0.58 & 0.08 & 0.01 & 0.02 & 0.00 \end{bmatrix}, \tag{21}$$

where $\omega_{k,LQR}$ is given in Hz.

Similarly, the concurrent design resulted in the following control gains

$$K_{opt} = \begin{bmatrix} 13.15 & -9.9 \\ 0.0 & 0.0 \\ 0.70 & 3.61 \\ -0.84 & 37.40 \\ 0.0 & 0.0 \\ 0.28 & -13.88 \\ 5.11 & -1.18 \\ 0.0 & 0.0 \\ 0.35 & 1.6 \\ -0.16 & 8.64 \\ 0.0 & 0.0 \\ 0.14 & -1.42 \end{bmatrix}, \tag{22}$$

where the resulting closed-loop dynamic characteristics are

$$\begin{bmatrix} \omega_{k,opt} \\ \zeta_{k,opt} \end{bmatrix} = \begin{bmatrix} 0.44 & 0.55 & 0.78 & 2.38 & 8.03 & 21.97 \\ 0.45 & 0.60 & 0.07 & 0.02 & 0.04 & 0.01 \end{bmatrix}. \tag{23}$$

A four-mode convolved ZV shaper for the low modes is chosen to eliminate the command-induced vibration. Its impulse sequence is given by

$$[A_i \ t_i] = \begin{bmatrix} 0.00 & 0.22 \\ 0.21 & 0.20 \\ 0.64 & 0.18 \\ 0.85 & 0.16 \\ 1.14 & 0.02 \\ 1.26 & 0.04 \\ 1.35 & 0.02 \\ 1.47 & 0.04 \\ 1.78 & 0.02 \\ 1.90 & 0.04 \\ 1.99 & 0.02 \\ 2.11 & 0.04 \end{bmatrix}, \tag{24}$$

and the resulting sensitivity curve subject to variations in ζ and natural frequency ω is shown in Fig. 5. The three lowest shaped modes are near one another, resulting in very low vibration in the range $0.4 < \omega < 0.8$. The fourth mode is the most lightly damped, and the point of zero vibration can be seen at $(\omega = 2.4, \zeta \approx 0)$. The shaping sequence results in near zero vibration for all frequencies where $\zeta > 0.2$.

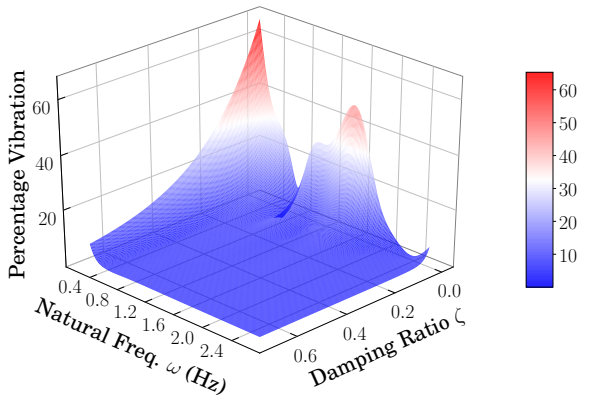

Fig. 5. Sensitivity curve of the multi-mode input shaper

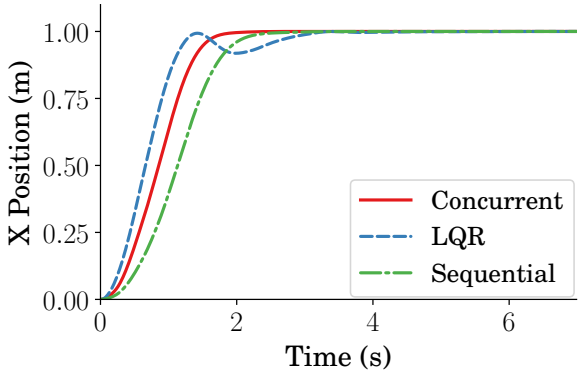

Fig. 6. Payload x-coordinate response

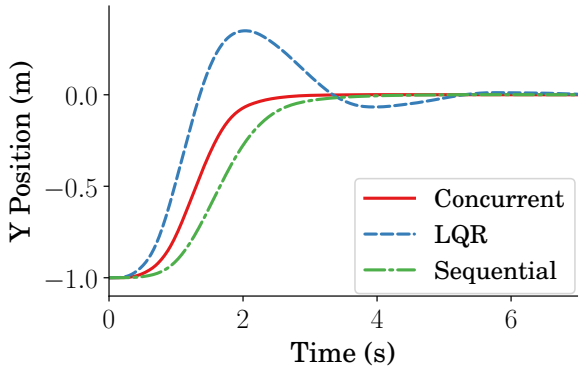

Fig. 7. Payload y-coordinate response

5.1 Optimized Command

To demonstrate the best-case performance of the proposed controller, a step command of amplitude $\Delta\theta_1 = \Delta\theta_2 = 90°$ starting from $\theta_1 = \theta_2 = 0$ was simulated for a system with the values in Table 1. To show a thorough comparison of the control methods, a sequentially designed LQR and shaped command was simulated in addition to the concurrently designed controller and LQR without shaping.

The system response to these commands is given in Figs. 6 and 7. These figures show the response of x and y payload coordinates for each control method. Although the LQR controller has a faster rise time than the concurrently designed command, it exhibits overshoot and requires time to dampen the resulting vibration. The shaped command effectively executes the desired motion without exciting unwanted vibration, resulting in a longer rise time, but shorter settling time. The sequentially designed command performs similarly to the concurrent controller, but with slower rise time.

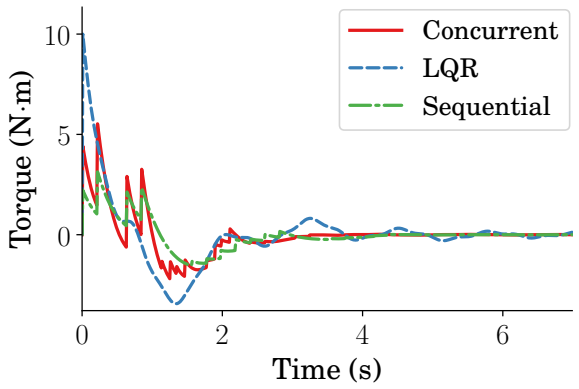

Fig. 8. Actuator 1 torque

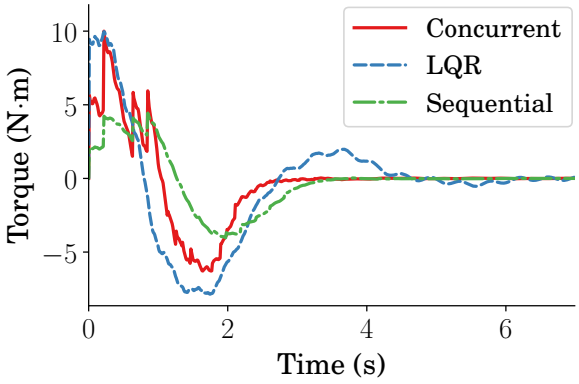

Fig. 9. Actuator 2 torque

The simulated actuator effort for both links is given in Figs. 8 and 9. Both simulations limit actuator effort at 10N·m. Because the input shaper breaks the reference command into a series of steps, it can utilize the full available torque more effectively than LQR alone. In comparison, the LQR controller yields high torque at the start of the command, while slowly damping over time. Because the sequential design does not use the full available torque, its command duration is longer than the concurrent design. The total energy consumed by the shaped command, measured by the absolute value of the definite integral from $t = 0$ to $t = 6$ of $u(t)$, is approximately 61% of the comparable LQR command, demonstrating the energy efficiency of the input shaping method.

Finally, the disturbance rejection properties of the proposed control method are compared to LQR in Fig. 10. In this figure, a positive amplitude force pulse of 20N is applied to the payload of the fully extended two-link arm. Because the concurrent design can have more aggressive control gains, it is more effective at damping the force disturbance than the benchmark LQR controller.

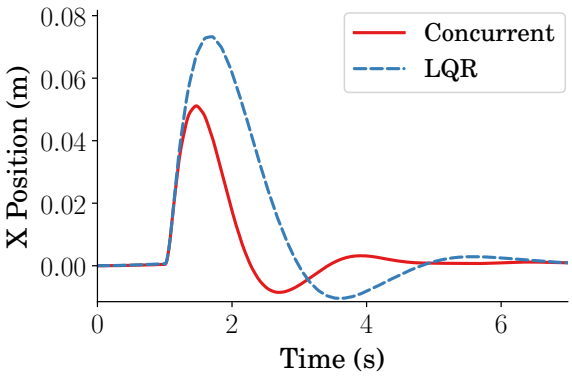

Fig. 10. Response to a force disturbance

6. CONCLUSION

This paper has presented a method for concurrently designing a linear control law with a multi-mode input shaper. The two-link flexible manipulator is used as a benchmark system for simulating this control law. When subject to a step input, the concurrently designed controller results in similar residual vibration while utilizing significantly less energy than LQR control. Furthermore, due to the more aggressive control gains allowed by the concurrent design, better disturbance rejection was attained.

REFERENCES

Baheri, A. and Vaughan, J. (2015). Concurrent design of unity-magnitude input shapers and proportional-derivative feedback controllers. In *American Control Conference (ACC)*, 1211–1216. IEEE.

Chatlatanagulchai, W. and Benjalersyarnon, T. (2015). Closed-loop input shaping with quantitative feedback controller applied to slewed two-staged pendulum. *Walailak Journal of Science and Technology (WJST)*, 13(8), 595–613.

De Luca, A. and Siciliano, B. (1991). Closed-form dynamic model of planar multilink lightweight robots. *IEEE Transactions on Systems, Man, and Cybernetics*, 21(4), 826–839.

Huey, J.R. and Singhose, W. (2010). Trends in the stability properties of clss controllers: A root-locus analysis. *IEEE Transactions on Control Systems Technology*, 18(5), 1044–1056.

Huey, J.R., Sorensen, K.L., and Singhose, W.E. (2008). Useful applications of closed-loop signal shaping controllers. *Control Engineering Practice*, 16(7), 836–846. doi:10.1016/j.conengprac.2007.09.004.

Huey, J. and Singhose, W. (2012). Design of proportional–derivative feedback and input shaping for control of inertia plants. *IET control theory & applications*, 6(3), 357–364.

Kapila, V., Tzes, A., and Yan, Q. (1999). Closed-loop input shaping for flexible structures using time-delay control. In *Conference on Decision and Control*, volume 2, 1561–1566. IEEE.

Kenison, M. and Singhose, W. (2002). Concurrent design of input shaping and proportional plus derivative feedback control. *Journal of Dynamic Systems, Measurement, and Control*, 124(3), 398–405.

Meurer, A., Smith, C.P., Paprocki, M., Čertík, O., Kirpichev, S.B., Rocklin, M., Kumar, A., Ivanov, S., Moore, J.K., Singh, S., Rathnayake, T., Vig, S., Granger, B.E., Muller, R.P., Bonazzi, F., Gupta, H., Vats, S., Johansson, F., Pedregosa, F., Curry, M.J., Terrel, A.R., Roučka, v., Saboo, A., Fernando, I., Kulal, S., Cimrman, R., and Scopatz, A. (2017). Sympy: symbolic computing in python. *PeerJ Computer Science*, 3, e103. doi:10.7717/peerj-cs.103.

Muenchhof, M. and Singh, T. (2002). Concurrent feed-forward/feed-back design for flexible structures. In *AIAA Guidance, Navigation and Control Conference,(Monterey, Ca.)*.

Singer, N.C. and Seering, W.P. (1990). Preshaping command inputs to reduce system vibration. *Journal of Dynamic Systems, Measurement, and Control*, 112(1), 76–82.

Singhose, W., Crain, E., and Seering, W. (1997). Convolved and simultaneous two-mode input shapers. *Control Theory And Applications*, 144(6), 515–520.

Singhose, W. (2009). Command shaping for flexible systems: A review of the first 50 years. *International Journal of Precision Engineering and Manufacturing*, 10(4), 153–168.

Smith, O.J. (1957). Posicast control of damped oscillatory systems. *Proceedings of the IRE*, 45(9), 1249–1255.

Sorensen, K.L., Singhose, W., and Dickerson, S. (2007). A controller enabling precise positioning and sway reduction in bridge and gantry cranes. *Control Engineering Practice*, 15(7), 825–837.

Staehlin, U. and Singh, T. (2003). Design of closed-loop input shaping controllers. In *American Control Conference*, volume 6, 5167–5172. IEEE.

Stergiopoulos, J. and Tzes, A. (2010). H closed-loop control for uncertain discrete input-shaped systems. *Journal of Dynamic Systems, Measurement, and Control*, 132(4), 041007.

Vaughan, J., Yano, A., and Singhose, W. (2008). Comparison of robust input shapers. *Journal of Sound and Vibration*, 315(4), 797–815.

Vyhlídal, T., Hromčík, M., Kučera, V., and Anderle, M. (2016). On feedback architectures with zero-vibration signal shapers. *IEEE Transactions on Automatic control*, 61(8), 2049–2064.

Yang, M.J., Gu, G.Y., and Zhu, L.M. (2014). High-bandwidth tracking control of piezo-actuated nanopositioning stages using closed-loop input shaper. *Mechatronics*, 24(6), 724–733.